

Molecular interactions of *Andrographis paniculata* Burm. f. Active Compound with Nuclear Receptor (CAR and PXR): An In Silico Assessment Approach

Elza Sundhani^{1,2}, Agung Endro Nugroho^{3*}, Arief Nurrochmad³, and Endang Lukitaningsih⁴

¹Doctoral Program in Pharmaceutical Science, Faculty of Pharmacy, Universitas Gadjah Mada, Yogyakarta 55281, Indonesia

²Department of Pharmacology and Clinical Pharmacy, Faculty of Pharmacy, Universitas Muhammadiyah Purwokerto, Jl. KH. Ahmad Dahlan Dukuwaluh, Purwokerto 53182, Central Java, Indonesia

³Department of Pharmacology and Clinical Pharmacy, Faculty of Pharmacy, Universitas Gadjah Mada, Sekip Utara, Yogyakarta 55281, Indonesia

⁴Department of Pharmaceutical Chemistry, Faculty of Pharmacy, Universitas Gadjah Mada, Yogyakarta 55281, Indonesia

* **Corresponding author:**

tel: +62-85643929723

email: nugroho_ae@ugm.ac.id

Received: July 27, 2021

Accepted: October 10, 2021

DOI: 10.22146/ijc.67981

Abstract: The study aims to analyze the potential Herb-Drug Interactions (HDIs) of the chemical compound in *Andrographis paniculata* Burm. f. against Constitutive Androstane Receptor (CAR) and Pregnane X Receptor (PXR). The 1XVP and 1SKX obtained from the Protein Data Bank (PDB) were used as the targeted protein. The molecular docking analysis was done using the Molecular Operating Environment (MOE) and molecular dynamics simulation using Gromacs. The results of the docking analysis showed that 14-Deoxy-11,12-didehydroandrographolide had the strongest binding energy (1XVP-21.0998 Å) with the Arene-H binding type on Tyr326 and Andrographidine A had the strongest binding energy (1SKX-24.7363 Å) with the Arene-H binding type on Trp299. While Andrographolide is the major component, it also has a high affinity for the two PDB IDs (1XVP-17.4044 Å and 1SKX-21.8881 Å). Based on the RMSD value, the radius of gyration (Rg), and MM/PBSA on molecular dynamic simulations, it shows that the ligand and protein complex as a whole can bind strongly to amino acid residues at the active site. The complex also has sufficient stability and good affinity. Therefore, this study can predict the mechanism in HDIs, especially in CYP 450 expression through the activation pathways of CAR and PXR receptors.

Keywords: *Andrographis paniculata*; CAR; PXR; 1XVP; 1SKX

■ INTRODUCTION

Herb-drug interaction (HDI) is one type of interaction that can cause problems in therapy. Herbal products contain secondary metabolites that have several pharmacological activities. Therefore, the concurrent use of herbal products with conventional drugs can cause Herb-Drug pharmacodynamic and pharmacokinetic interactions at risk of causing adverse effects [1-2]. Interactions between herbs and drugs in the pharmacokinetics phase, particularly metabolism, have been shown to have a substantial impact. For example, plasma, tissue, and urine drug levels can be affected by

interactions with herbs with drug-metabolizing enzyme complexes (cytochrome P450) [3-4].

Constitutive Androstane Receptor (CAR) and Pregnane X Receptor (PXR) are a group of nuclear receptors (orphan nuclear receptor subfamily) that play a role in the expression of several metabolizing enzymes [5]. CAR and PXR have several cytochrome P450 gene targets such as CYP3A1, CYP3A4, CYP3A5, CYP3A7, CYP2A6, CYP2B6, CYP2C8, CYP2C9, CYP2C19, CYP4F12, CYP27A1, as well as phase 2 conjugate enzymes (UGT-UG1, UGT1, UGT1A4, UGT1A6, and UGT1A9), sulfotransferases (Sult2a1), glutathione S-transferases (Gsta2 and GSTA4), and carboxylesterases

which play an essential role in the process of drug metabolism [6-7]. Thus, changes in the expression of drug metabolism genes mediated by CAR/RXR and PXR/RXR heterodimers can cause serious drug-drug/herb-drug interactions by enhancing the metabolism of other drugs [8].

Sambiloto (*Andrographis paniculata* Burm. f.) is a widely used plant as traditional medicinal in Asian countries such as China, Japan, Malaysia, Bangladesh, India, Thailand, and Indonesia [9]. The pharmacological effects of this plant include anti-inflammatory, antimalarial, antiviral, antibacterial, immune-suppressive, cardio and hepatoprotective, antidiabetic, antiobesity, and anticancer [10-12]. Herb-drug interactions have been observed when Sambiloto is used as a supplementary therapy with medicinal components. Based on previous studies, several characteristics of pharmacokinetics and pharmacological activities of several drugs such as theophylline, etoricoxib, and naproxen experienced significant changes after being combined with Sambiloto extract [13-15]. Sambiloto extracts and Andrographolide have proven to inhibit the kinetics of the CYP2E1 enzyme and reduce the expression of CYP2C and CYP3A proteins [16-19]. In contrast, the content of 14-Deoxy-11,12-didehydroandro-grapholide in Sambiloto was also reported to inhibit the expression of CYP3A4 protein [20].

Scientific evidence based on *in vitro* and *in vivo* test results from the active compounds of the Sambiloto plant shows that it has the potential to cause interactions if used together with drugs, especially in the metabolic phase involving the CYP 450 enzyme. The chemical compound in Sambiloto includes Andrographolide, Neoandrographolide, 14-Deoxyandrographolide, 14-Deoxy-11,12-didehydroandrographolide, Andrographiside, Andrographidine A, and derivatives of other compounds are thought to play a role in determining its pharmacological activity and herb-drugs interaction [12,21-22]. The secondary metabolite in Sambiloto is thought to have the potential to cause interactions with several drugs considering their high use in the community. Still, it is not known as the mechanism of involvement of the CAR and PXR receptors. Based on the literature study, there was no study of the mechanism of chemical substances in Sambiloto on the activation of

CAR and PXR receptors. The *in silico* study using molecular docking will predict the binding energy between chemical constituents of Sambiloto with CAR and PXR receptors.

In silico studies using CAR and PXR receptor targets have been widely used to predict drug-drug interactions or herb-drug interactions. Several isolated compounds from Chinese herbal medicines have been proven to activate the regulation of PXR (2QNV) and CYP3A4 through an *in silico* docking molecular study similar to the results of *in vitro* studies on HepG2 and Huh7 cells [23]. The metabolic mechanisms in CAR and PXR receptor activation pathways using molecular docking studies can predict molecular mechanisms on the animal study [6,24,25]. The results from molecular docking were then evaluated using molecular dynamics simulations to investigate stability, hydrogen bond occupancy, and binding free energy of ligands and proteins in an aqueous system. The results of this study are expected to be used to predict the mechanism of herb-drug interaction through the CAR-PXR receptor activation pathway.

■ EXPERIMENTAL SECTION

Materials

The target CAR (Constitutive Androstane Receptor) PDB IDs in the study are 1XVP (Complex of Human CAR/RXR heterodimer bound with CITCO) and 1XV9 (Complex of Human CAR/RXR heterodimer bound with SRC1 peptide, fatty acid, and 5b-pregnane-3,20-dione).

The PDB IDs are PXR (Pregnane X Receptor) receptors such as 1SKX (Complex of Human PXR and the Macrolide Antibiotic Rifampicin); 2QNV (Pregnane X Receptor bound to Colupulone); 3R8D (Human Nuclear Xenobiotic Receptor PXR by the Reverse Transcriptase-Targeted Anti-HIV Drug PNU-142721); 4NY9 (Human PXR-LBD In Complex with N-{(2R)-1-[(4S)-4-(4-chloro phenyl)-4-hydroxy-3,3-dimethylpiperidin-1-yl]-3-methyl-1-oxobutan-2-yl}-3-hydroxy-methyl butanamide). All of the PDB IDs were obtained from the protein data bank website (<https://www.rcsb.org/>).

The ligands used in this study were 11 chemical constituents from Sambiloto (Table 1), agonist ligand

1XVP (Phenytoin) dan agonist ligand 1SKX (hyperforin) collected from Pubchem, then drawn on Chemdraw Ultra 12.0.

Instrumentation

In silico molecular docking studies using Molecular Operating Environment (MOE) version 2010.10 (developed by Chemical Computing Group Inc, Canada), operated using HP 13-AN1033TU Notebook Windows 10 Home with an Intel® Core™ i3-1005G1 processor with 512 GB SSD storage capacity and 8 GB memory. Molecular dynamics simulation to the molecular docking the result used AnteChamber PYthon Parser interfacE (ACPYPE), Gromacs 2016.3, g_mmpbsa package, and VMD 1.9.3 [26,27], which is operated using a computer with Intel (R) Core i5-8500 CPU@4.30GHz (6 CPUs) processor, 4096 MB RAM, 2 TB hard drive, 120 GB solid-state drive, NVIDIA GeForce GTX 1080 Ti.

Procedure

Ligands preparation

The chemical structures from Phenytoin (Agonist CAR receptor), Hyperforin (Agonist PXR receptor), and chemical constituents of *Andrographis paniculata* Burm. f. were drawn using the builder feature in MOE. First, the hydrogen atom was added with protonate 3D and charged with partial charges, and then the energy was minimized to give the most stable conformation.

Preparation of CAR and PXR receptor

All crystal structures for molecular docking were prepared using MOE software. The protein structure was prepared by removing the water molecule and adding hydrogen atoms with protonate 3D, being charged with partial charges, and correcting errors by quick-prep on the structure of each protein ID.

Validation of docking method

The validation of the docking method was begun by finding the binding target in the specific area of the CAR and PXR receptor target proteins, respectively. The validation process was based on the Root Mean Square Deviation (RMSD) value. The RMSD value is $< 2 \text{ \AA}$ to ensure the best docking position between the ligand and the protein. Each CAR and PXR receptor ID obtained

from PDB validity was tested by using the native ligand from each receptor at different positions. Each position was replicated ten times to get RMSD values less than 2 \AA . Placement methods from the molecular docking with MOE software using *Triangle Mather*, refinement method using *forcefield*, and scoring method using *London DG* are selected to optimize the docking method that produces the best RMSD value.

Molecular docking analysis

Molecular docking of constituents of *Andrographis paniculata* Burm. f. (Table 1) and the receptor agonist was carried out at proper binding positions of target receptors. Observation of the ligand poses to predict interactions, binding modes, and overlapping structures and the docking score to estimate affinity was used in the research. The molecular docking score describes the strength of the interaction between the ligand and the receptor and can predict the quantity of bond energy. The lower the binding energy value from the molecular docking results, the more stable and more robust the bond between the ligand and the receptor can describe the higher affinity for the ligand to its target receptor [28-29].

Molecular dynamics simulation

The AMBER14SB force field was used to describe the protein in this molecular dynamics study. The ligand parameterization and calculation of the long-range electrostatic force employed the AnteChamber PYthon Parser interface (ACPYPE) and Particle Mesh Ewald method, respectively [27]. The system from molecular dynamics was neutralized by adding Na^+ and Cl^- ions. These systems were solvated in explicit TIP3P water model.

Berendsen thermostats and barostats are used during the heating stage, with the pressure being maintained at 1 bar. The simulation steps included minimization until 500000 steps, heating until 310 K, temperature equilibration (NVT) in 500 ps, pressure equilibration (NPT) in 500 ps, and a production run with a 2 fs time step for 100 ns. Data analysis has been carried out in the form of Root Mean Square Deviation (RMSD), Root Mean Square Fluctuation (RMSF), Radius

Table 1. Chemical constituents of *Andrographis paniculata* taken by ChemDraw Ultra 12.0.2.1076 [9]

No	Compound	Structure	No	Compound	Structure
1	14-Deoxy-11,12-didehydroandrographolide		7	Andrographidine A	
2	14-Deoxy-11-hydroxyandrographolide		8	Andrographidine C	
3	14-Deoxy-12-hydroxyandrographolide		9	Andrographolactone	
4	14-Deoxyandrographolide		10	Andrographolide	
5	8,17-Epoxy-14-Deoxyandrographolide		11	Neoandrographolide	
6	Andrograpanin				

of Gyration (R_g), Solvent-Accessible Surface Area (SASA), Radial Distribution Function (RDF), and hydrogen bond analysis (HBond).

MM/PBSA calculation

MM/PBSA calculation was performed using the `g_mmpbsa` within the Gromacs 2016.3 software [26]. Polar desolvation energy was calculated with the Poisson-Boltzmann equation with a grid size of 0.5 Å. The dielectric constant of the solvent was set to 80 to represent water as the solvent. The non-polar contribution was determined by calculating the solvent-accessible surface area (SASA) with the radii of the solvent as 1.4 Å. Finally, the binding free energy of the complex was determined based on 50 snapshots taken from the beginning to the end of the molecular dynamics simulation trajectories of the complex.

RESULTS AND DISCUSSION

The docking results of several PDB IDs for the CAR (1XVP & 1XV9) and PXR (1SKX, 2QNV, 3R8D, & 4NY9) receptors showed that 1XVP, 1SKX, and 4NY9 had the criteria for the RMSD value < 2 Å. The RMSD value according to these criteria indicated that the ligand position did not change significantly after the docking procedure. Based on the docking score, 1XVP and 1SKX have the best scores. The negative value shows intense binding energy and describes the greater affinity between the ligand and protein (Table 2). Thus, there are 1XVP

and 1SKX, which have been selected for molecular docking studies with the chemical compounds in Sambiloto.

CITCO (native ligand of 1XVP) is the activator of human CAR. CITCO induce the expression of several phases I metabolizing enzymes (CYP2B6, CYP3A4, CYP2C8) and Phase II conjugation genes such as (SULT1A1, GSTA2, MDR1) [30]. Rifampicin is the native ligand of the ID 1SKX Protein, PXR receptor agonist, and an activator of some genes phase I and II metabolizing enzymes. Rifampicin targets the activation of the metabolizing enzyme gene through the PXR pathway, including CYP2B6, CYP2C8, CYP2C9, CYP2C19, CYP3A4, UGTs, and GSTs [31]. The macrolide ring in Rifampicin binds via several amino acids 178–209 and 229–235 on PXR ligand-binding pockets [32]. These amino acids are appropriate with the docking analysis for validating Rifampicin as a native ligand bound to the amino acids Phe 288 and Trp299 from 1SKX.

The molecular docking of Sambiloto chemical compounds on 1XVP and 1SKX proteins (Table 3) indicates that all compounds have an affinity for one or both proteins, as indicated by the more negative values of binding energy. Binding energy or docking score shows the strength of the bond between the ligand and the macromolecule or protein. The negative value binding energy indicates the solid and stability of the binding

Table 2. Result of the docking procedures validation for several PDB IDs of CAR and PXR receptor with native ligand

Receptor	PDB ID	Co-crystallized Ligand (native ligand)	Docking Score	RMSD (Å)	Ligand Atom	Amino Acid	Binding type	Distance (Å)
CAR	1XVP	CITCO	-29.3242	1.3640	C	Phe234	Arene-H	3.96
					C	Phe217	Arene-H	3.91
	1XV9	5b-pregnane-3,20-dione	-	-	-	-	-	-
PXR	1SKX	Rifampicin	-33.9689	1.2470	C	Phe288	Arene-H	4.10
					C	Trp 299	Arene-H	3.88
					C	Trp 299	Arene-H	3.60
	2QNV	Colupulone	-17.7709	5.4224	-	-	-	-
	3R8D	PNU-142721	-22.5619	6.9041	C	Phe288	Arene-Arene	3.85
	4NY9	N-[(2R)-1-[(4S)-4-(4-chlorophenyl)-4-hydroxy-3,3-dimethylpiperidin-1-yl]-3-methyl-1-oxobutan-2-yl]-3-hydroxy-methylbutanamide	-24.7378	1.1088	C	Leu240	Arene-H	4.48

Table 3. Molecular docking results of *Andrographis paniculata* chemical compound against protein 1XVP and 1SKX

No	Compound	1XVP					
		Docking Score	RMSD-Refine (Å)	Ligand Atom	Amino Acid	Binding type	Distance (Å)
1	14-Deoxy-11,12-didehydroandrographolide	-21.0998	1.4344	C	Tyr326	Arene-H	4.40
2	14-Deoxy-11-hydroxyandrographolide	-13.5205	0.5966	C	Tyr326	Arene-H	3.95
3	14-Deoxy-12-hydroxyandrographolide	-15.6392	0.8061	C	Tyr224	Arene-H	3.48
4	14-Deoxyandrographolide	-11.5683	1.4049	C	Phe234	Arene-H	4.14
5	8,17-Epoxy-14-Deoxyandrographolide	-15.9161	1.5090	C	Tyr224	Arene-H	3.48
6	Andrograpanin	-12.3822	1.1631	C	Phe234	Arene-H	3.96
7	Andrographidine A	-9.9899	1.0956	C	Leu206	Arene-H	3.82
8	Andrographidine C	-9.1853	1.8843	C	Phe161	Arene-H	4.34
				O	Phe161	Arene-H	3.99
9	Andrographolactone	-17.3880	1.7166	C	His203	Arene-H	3.92
10	Andrographolide	-17.4044	1.6933	C	Tyr326	Arene-H	4.61
11	Neoandrographolide	15.3878	1.1199	C	Tyr 224	Arene-H	3.82
12	Agonist ligand	-18.6943	1.2352	N	Phe217	Arene-H	4.15
				C	Phe161	Arene-H	3.97

Table 3. Molecular docking results of *Andrographis paniculata* chemical compound against protein 1XVP and 1SKX (Continued)

No	Compound	1SKX					
		Docking Score	RMSD-Refine (Å)	Ligand Atom	Amino Acid	Binding type	Distance (Å)
1	14-Deoxy-11,12-didehydroandrographolide	-19.1904	1.5274	C	Phe288	Arene-H	4.32
				C	Trp299	Arene-H	4.39
2	14-Deoxy-11-hydroxyandrographolide	-22.7215	1.7104	C	Trp 299	Arene-H	3.88
				C	Phe288	Arene-H	3.71
3	14-Deoxy-12-hydroxyandrographolide	-19.8710	2.3171	C	Trp 299	Arene-H	4.27
				C	Phe288	Arene-H	4.46
4	14-Deoxyandrographolide	-21.6525	1.8951	C	Phe288	Arene-H	4.43
				C	Phe288	Arene-H	3.67
				C	Trp299	Arene-H	3.88
5	8,17-Epoxy-14-Deoxyandrographolide	-20.9802	3.7858	C	Trp 299	Arene-H	3.88
				C	Phe288	Arene-H	3.84
6	Andrograpanin	-19.1204	3.4365	C	Trp 299	Arene-H	4.00
				C	Phe288	Arene-H	4.37
7	Andrographidine A	-24.7363	1.8460	O	Trp 299	Arene-H	3.11
8	Andrographidine C	-24.4739	2.8105	O	Phe420	Arene-H	3.91
				C	Phe288	Arene-H	3.78
				C	Leu324	Arene-H	4.11
9	Andrographolactone	-21.0887	2.0251	C	Trp299	Arene-H	3.70
				C	Tyr306	Arene-H	3.60
10	Andrographolide	-21.8881	1.9172	C	Trp299	Arene-H	3.79
11	Neoandrographolide	-21.6999	1.9530	C	Phe288	Arene-H	3.47
				C	Tyr 306	Arene-H	3.74
12	Agonist ligand	-15.5579	1.5085	C	Trp 299	Arene-H	4.35

formed between the ligand and the receptor on the macromolecule [26,33].

Each compound has explicitly binding sites on the amino acid target protein on Phe 234; Phe217 (1XVP), and the binding site on Phe288; Trp 299; Trp 299 (1SKX). 14-Deoxyandrographolide and Andrograpanin have bonded to Phe 234, such as the 1SKX native ligand on the

C atom (Arene-H), while the Agonist ligand (Phenytoin) binds explicitly to N-Phe217 and Phe 161 (Arene-H) (Fig. 1 and 2). The compound 14-Deoxy-11,12-didehydro-andrographolide and Andrographolide had the most potent binding energy value against 1XVP. The lactone rings present in these two compounds play a role in determining the bond with Tyr326 in the 1XVP protein.

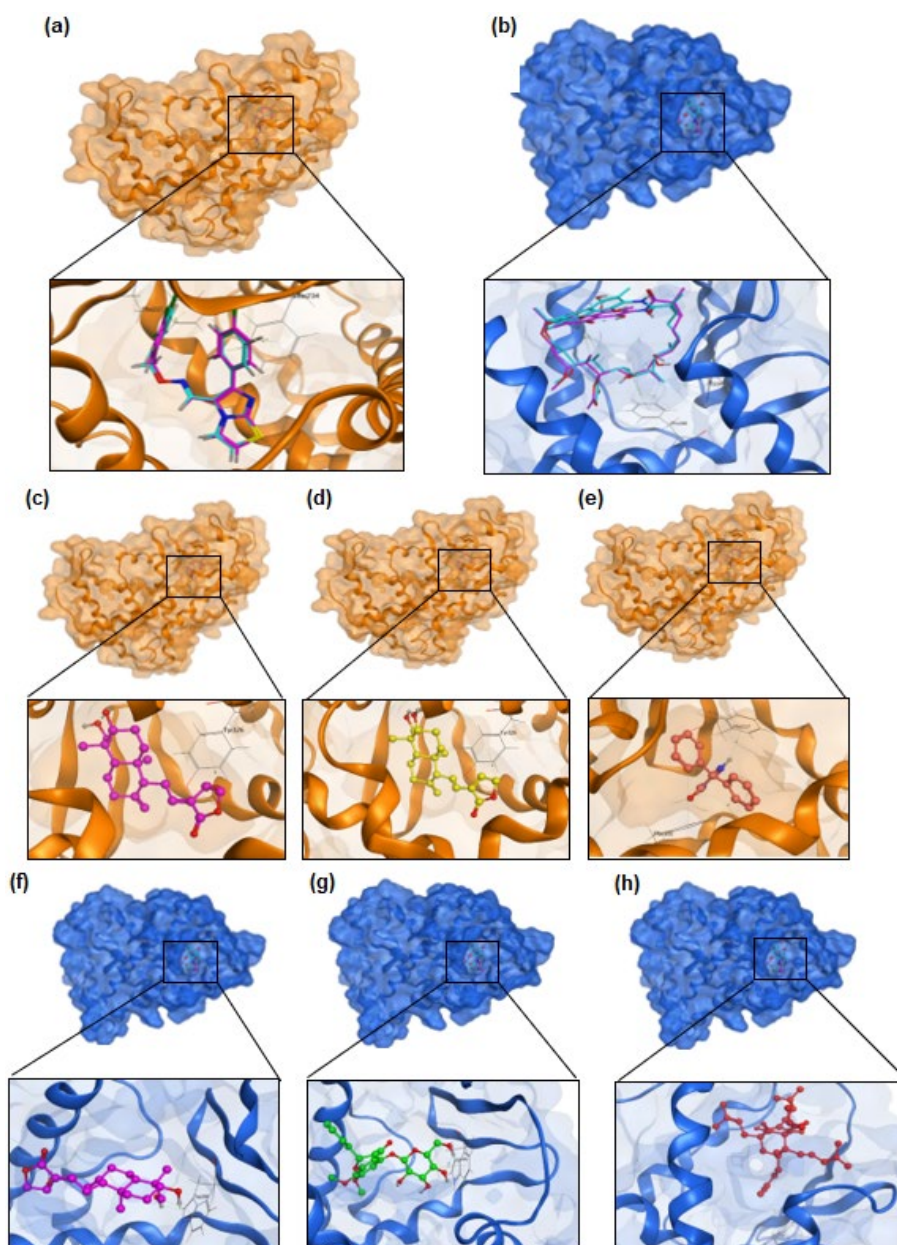


Fig 1. 3D-Conformation ligand position redocking with the proposed procedure: (a) 1XVP with CITCO (RMSD:1.364 Å) and; (b)1SKX with Rifampicin (RMSD: 1.247 Å) and ligand interaction Sambiloto chemical constituent to 1XVP and 1SKX using MOE. 1XVP-Andrographolide (c); 1XVP- 14-Deoxy-11,12-didehydroandrographolide (d); 1XVP agonist (e); 1SKX-Andrographolide (f); 1SKX- Andrographidine A (g); 1SKX-Agonist (h)

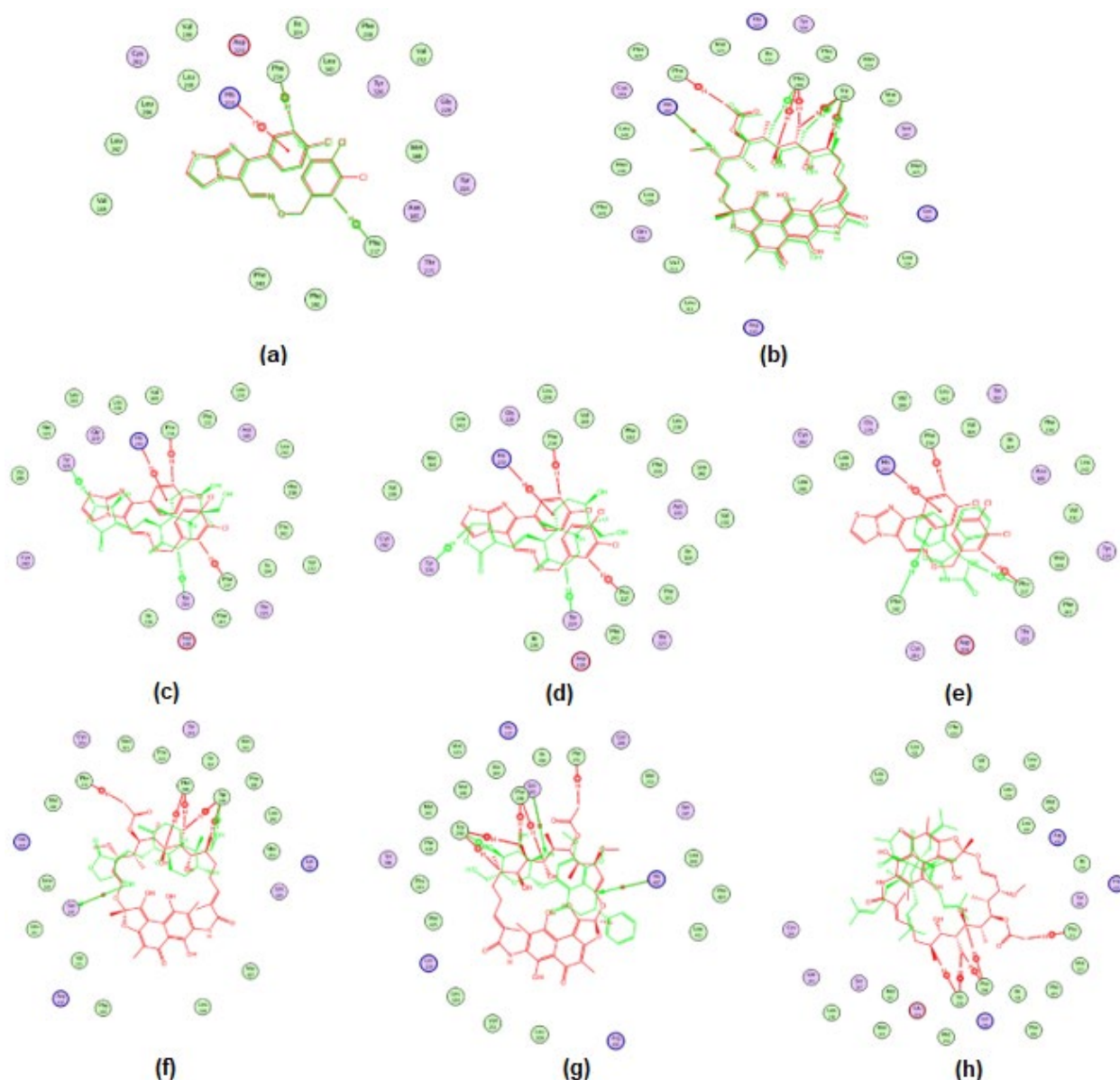


Fig 2. 2D-Conformation Ligand Position redocking with the proposed procedure: (a) 1XVP CITCO and; (b) 1SKX with Rifampicin, and ligand Interaction Sambiloto Chemical Constituent to 1XVP and 1SKX using MOE. 1XVP-Andrographolide (c); 1XVP- 14-Deoxy-11,12-didehydroandrographolide (d); 1XVP agonist (e) 1SKX-Andrographolide (f)1SKX- Andrographidine A (g) 1SKX-Agonist (h)

Even though it binds to the same amino acid residue, the binding energy of the Andrographolide is weaker than that of 14-Deoxy-11,12-didehydroandrographolide. Adding a hydroxyl group ($-OH$) to the lactone ring causes a decrease in the amount of Andrographolide binding energy in the protein.

14-Deoxyandrographolide and Andrograpanin compounds have lower bond energies compared to the

two previous compounds. However, both bind to the same amino acid as the native 1XVP ligand, namely the amino acid Phe234. In contrast, 14-Deoxy-11,12-didehydroandrographolide and Andrographolide do not attach to amino acids bound by native ligands. The different types of amino acids in 1XVP that bind to the compound structure of the Sambiloto plant indicate a difference in the binding sites between these compounds

and the native ligand. However, the affinity with 1XVP is quite strong, considering that the binding energy value is different from the native ligand. The chemical compound of the Sambiloto plant has been shown to have an affinity for the PXR receptor, especially for the 1SKX protein, which is indicated by its strong binding energy value and binds to one or two of the same amino acids as the native ligand, namely Phe288 and Trp299. Furthermore, Andrographidine A is proven being the most potent binding energy against 1SKX in Trp299 amino acid. Andrographolide, the main compound in the Sambiloto

plant, also binds to the same amino acid as the native ligand, Trp299.

Molecular dynamics simulation aims to identify the stability of the molecular interactions of each complex system by using the initial conformation of the molecular docking simulation results. Molecular dynamics captures the position and mobility of each atom at every second of time, allowing it to describe the behavior of proteins and other biomolecules in atomic detail. In addition, molecular dynamics simulations can be carried out under controlled conditions (initial protein

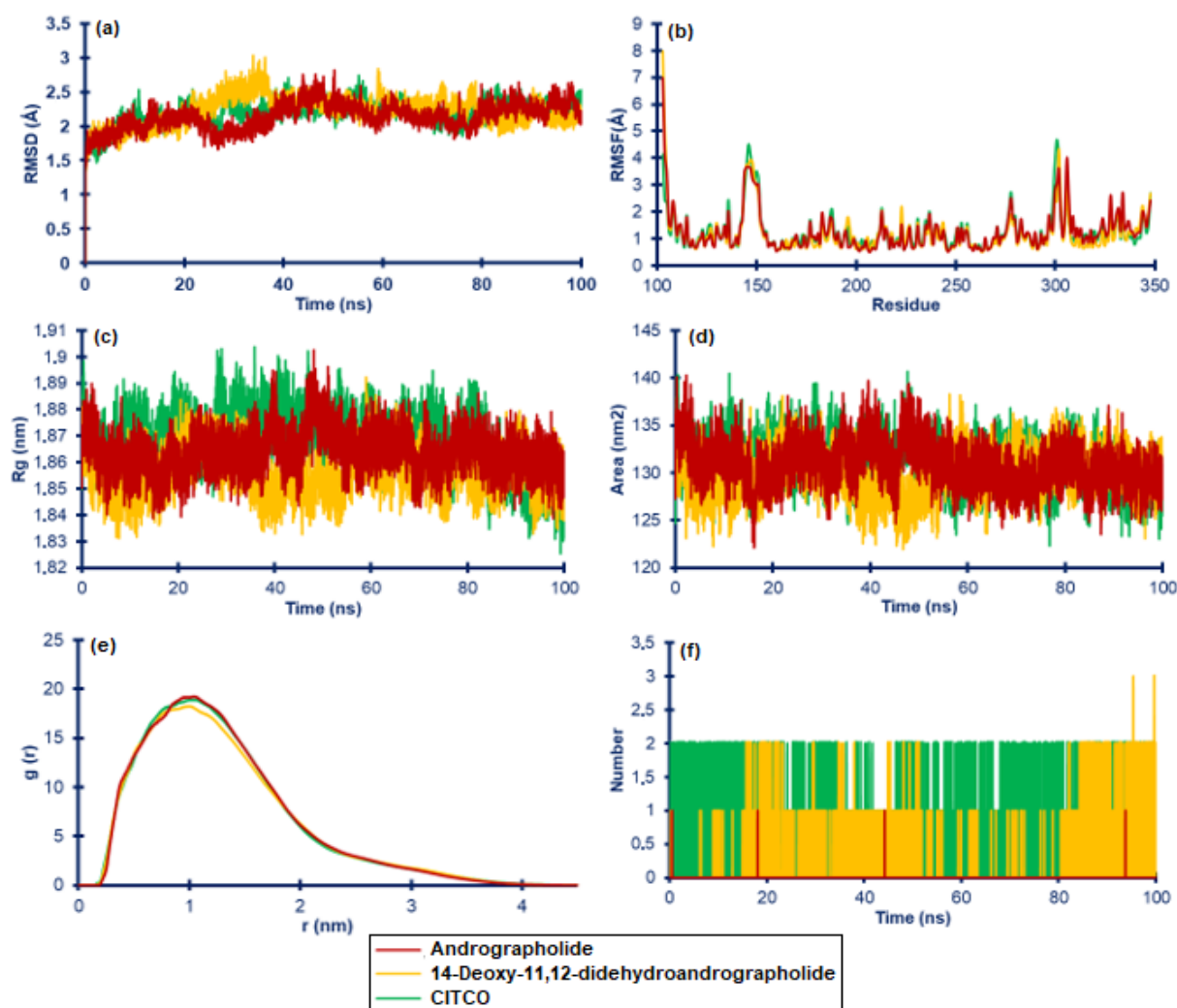


Fig 3. The molecular dynamics simulation results of complex Andrographolide, 14-Deoxy-11,12-didehydroandrographolide, and CITCO as native ligand with 1XVP. Root Mean Square Deviation (RMSD) (a); Root Mean Square Fluctuation (RMSF) (b); Radius of Gyration (Rg) (c); Solvent-Accessible Surface Area (SASA) (d); Radial Distribution Function (RDF) (e); and hydrogen bond analysis (HBond) (f)

conformation, bound ligand, post-translational mutation or modification, protonation state, temperature, and the voltage across the membrane) [34-35]. Based on snapshots taken at the beginning complex simulation with 1XVP and 1SKX (simulation), all compounds are rotated and translated during the simulation. Still, significant changes were shown by the 14-Deoxy-11,12-didehydroandrographolide-1XVP and Andrographolide-1SKX. These two compounds fluctuated and began to move away from the area of the active site of binding to the receptor macromolecule. The interaction dynamics between the compound and the target macromolecule were studied using molecular dynamics simulation in an explicit

solvent. Strong affinity tends to reduce the movement of bound atoms and will generally stabilize the active site of the receptor macromolecule [34,36]. This phenomenon can be analyzed by calculating the RMSD value of the target macromolecule during a 100 ns simulation to ensure the stability and rationality of the selected conformation. The RMSD graphs in Fig. 3 and 4 show that 14-Deoxy-11,12-didehydroandrographolide-1XVP (2.22 Å); Andrographolide-1XVP (2.19 Å) and Andrographolide-1SKX (3.80 Å); Andrographidine A-1SKX (3.13 Å) experienced significant fluctuations during the simulation. However, the RMSF graph shows a difference in results with the RMSD graph; the average

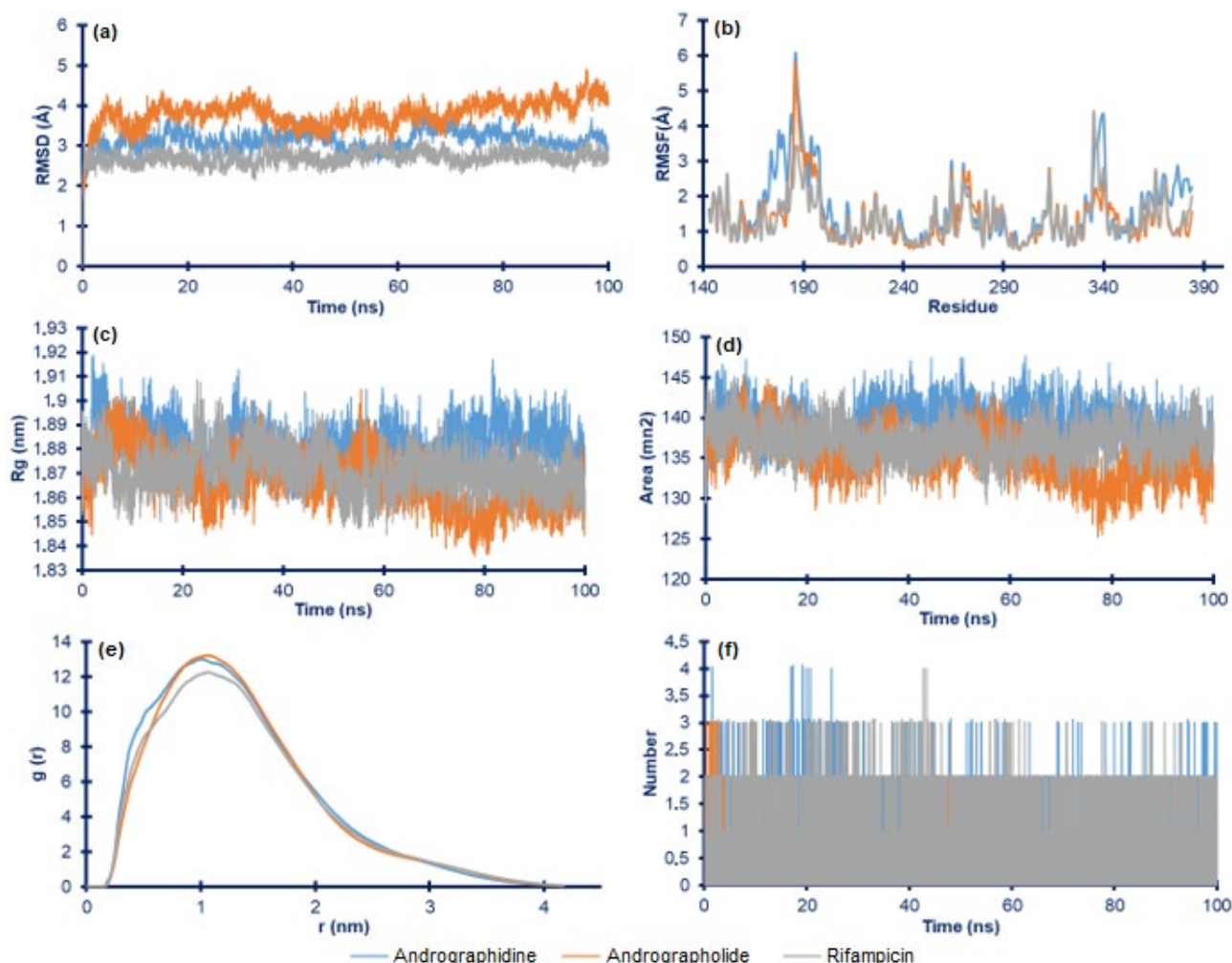


Fig 4. The molecular dynamics simulation results of complex Andrographidine A, Andrographolide, and Rifampicin as native ligand with 1SKX. Root Mean Square Deviation (RMSD) (a); Root Mean Square Fluctuation (RMSF) (b); Radius of Gyration (Rg) (c); Solvent-Accessible Surface Area (SASA) (d); Radial Distribution Function (RDF) (e); and hydrogen bond analysis (HBond) (f)

RMSF value of Andrographolide-1XVP (1.26 Å) and Andrographidine A-1SKX (1.64 Å) indicated the stability of the protein-ligand complex interaction, and the average value of the entire complex system can bind strongly with amino acid residues at the active site of binding of the receptor macromolecule [37].

Furthermore, identification of the radius of gyration (Rg) is carried out to determine the stability of the complex, whether the complex system is stable in folded or unfolded form during the simulation. The Rg value indicates an insignificant difference from the overall complex system. Observations on solvent-accessible surface area (SASA) were also carried out to predict the extent to which receptor macromolecules undergo conformational changes during simulations that are accessible to water molecules [38-39]. The results of the SASA analysis showed that Andrographolide-1XVP had a fairly high value of 131.21 nm², and Andrographidine A-1SKX had a higher average SASA value than other compounds, which was 139.44 nm². Then evaluation was carried out on the effect of each parameter variation on atomic density or probability at a certain radius using the radial distribution factor (RDF) (Fig. 3 and 4), which will illustrate the distribution of a molecule around another molecule giving the possibility of finding atomic pairs located at a distance of "r" [40-42]. The RDF value from 14-Deoxy-11,12-didehydroandrographolide-1XVP (6.27 g(r)) and Andrographolide-1XVP (6.23 g(r)) not much different with native ligand CITCO (6.26 g(r)). These results also occur in 1SKX complex (Andrographolide-1SKX (4.87 g(r)); Andrographidine A-1SKX (5.03 g(r)); and Rifampicin (4.73 g(r)). The results of H-bond calculations during the simulation showed fluctuations around amino acid residues located at the active binding site of receptor macromolecules. Then calculate the

number of hydrogen bonds between the test compound and receptor macromolecules during the molecular dynamics simulation. The high percentage of hydrogen bonds and hydrogen bond occupancy from this study indicates stability (Table 4). Total hydrogen bond and hydrogen bond occupancy determine the stability of each system and are the keys to the interaction stabilization of the protein-ligand complex [43].

Based on the MM/PBSA calculations results, all complexes with 1XVP and 1SKX showed good affinity. However, CITCO and Rifampicin as native ligands of each protein still had the best affinity, as indicated by the high value of total binding energy (ΔG_{bind}) represented in Table 5. The energies that contribute the most during the simulation are van der Waals, electrostatic, and non-polar interactions. This phenomenon is because the MM/PBSA approach allows the observation of van der Waals effects, electrostatic contributions, and changes in ligand-receptor affinity that are affected by the solvation process in complex systems [27,34,43].

Sambiloto chemical compound is a substrate of CYP450, which can act as an enzyme inductor or inhibitor. The inductor or inhibitor of the CYP450 enzyme can lead to potential herb-drug interactions when used in conjunction with conventional drugs. Based on *in silico* absorption, distribution, metabolism, and excretion (ADMET) analysis, Andrographolide, Neoandrographolide, 14-Deoxyandrographolide, and Andrographiside are substrates of CYP450, and most of them are absorbed through intestinal/positive HIA (Human Intestinal Absorption) scores [44]. Meanwhile, the SwissADME prediction study results show that deoxyandrographolide is a CYP2C9 inhibitor, and Andrographolactone is an inhibitor of CYP2C9 [45]. Furthermore, *in vitro* studies show that Andrographolide

Table 4. Hydrogen bond occupancy

PDB ID	Active Compound	Occupancy (%)
1XVP	Andrographolide	59.14 %
	14-Deoxy-11,12-didehydroandrographolide	34.48 %
	CITCO	0.04 %
1SKX	Andrographidine A	76.67 %
	Andrographolide	24.34 %
	Rifampicin	74.97 %

Table 5. Free bonding energy during molecular dynamics simulation

PDB ID	Active Compound	ΔE_{vdw} (kJ/mol)	ΔE_{ele} (kJ/mol)	ΔG_{PB} (kJ/mol)	ΔG_{NP} (kJ/mol)	ΔG_{Bind} (kJ/mol)
1XVP	Andrographolide	-217.66	-26.69	125.72	-19.31	-137.94
	14-Deoxy-11,12-didehydroandrographolide	-211.21	-16.92	98.93	-18.80	-147.99
	CITCO	-228.58	-8.41	107.43	-20.36	-149.93
1SKX	Andrographidine A	-224.45	-53.52	161.16	-22.54	-159.35
	Andrographolide	-108.34	-32.49	119.40	-18.44	-108.86
	Rifampicin	-335.15	-46.52	172.72	-31.16	-240.11

ΔE_{vdw} = van der Waals contribution

ΔE_{ele} = electrostatic contribution

ΔG_{PB} = polar contribution of desolvation

ΔG_{NP} = non-polar contribution of desolvation

Table 6. *In vitro* activity of cytochrome P450s expression from *Andrographis paniculata* Burm. f. active compound

No	Active Compound	Expression Cytochrome P450s		Reference
		Increased	Decreased	
1	Andrographolide	nd	(CYP1A2, CYP2D6, CYP3A4) ^{*1}	[20]
		nd	(CYP3A4) ^{*2}	[19]
		nd	(CYP3A, CYP2C) ^{*3}	[17]
2	14-Deoxy-11,12-didehydroandrographolide	nd	(CYP1A2, CYP2D6, CYP3A4) ^{*1}	[20]
3	Andrographidine A	nd	nd	

^{*1} protein expressions of cytochrome P450s in HepG2 hepatoma cells

^{*2} protein expressions of cytochrome P450s in modified Caco-2 cells

^{*3} hepatic cytochrome P450 mRNA expression on human hepatocyte cultures

nd means no data

plays a significant role in herb-drug interactions by inhibiting several CYP450 enzyme families (Table 6). This fact is consistent with the results of molecular docking analyses on CAR and PXR that Andrographolide has high binding energy in the two target proteins.

As the primary compound in Sambiloto, Andrographolide is known to play a role in determining pharmacological activity and potential herb-drug interaction. This interaction is widely evidenced in the antidiabetic activity of the bitter herb extract and Andrographolide which has been shown to have antihyperglycemic activity in a rat model of type 2 diabetes by repairing pancreatic beta cells and increasing GLUT-4 translocation [46-47]. The combination of Andrographolide with several oral antidiabetic drugs such as metformin, glimepiride, and glyburide can increase the antihyperglycemic effect compared to a single administration, which is in line with the increase in pharmacokinetic parameters C_{max} and AUC [48]. In

addition, Andrographolide can change the pharmacokinetic parameters of other drugs such as etoricoxib by lowering C_{max} , AUC, TT values and increasing Vd and CL, which affect the anti-inflammatory activity of etoricoxib [14]. The pharmacokinetic profile and pharmacological action of Naproxen and Warfarin also changed due to co-administration with Andrographolide [13,49].

■ CONCLUSION

Based on *in silico* studies, it is proven that the compounds in Sambiloto (*Andrographis paniculata* Burm. f.), especially 14-Deoxy-11,12-didehydroandrographolide, Andrographidine A, and Andrographolide had the most potent binding energy for the nuclear receptors (CAR and PXR). Furthermore, molecular dynamics simulations show that all complexes of these compounds and receptors have good affinity and are sufficient stability. Therefore, although

it must be proven through *in vitro* and *in vivo* studies, this study is adequate to predict the mechanism of herb-drug interactions (HDIs) from Sambiloto to several drug metabolism via CYP450 through the activation pathways of CAR and PXR receptors.

■ ACKNOWLEDGMENTS

The author would like to acknowledge the funding support for molecular docking analysis from UGM No. 49.01.02/UN1/FFA1/SET.PIM/PT/2021 and molecular dynamics simulation from UGM No. 3143/UN1.P.III/DIT-LIT/PT/2021.

■ AUTHOR CONTRIBUTIONS

Elza Sundhani, Agung Endro Nugroho, Arief Nurrochmad, Endang Lukitaningsih conducted the experiment. Elza Sundhani wrote the manuscript and conducted the scoring docking analysis and simulation of dynamical molecules. Agung Endro Nugroho, Arief Nurrochmad, and Endang Lukitaningsih supervision of the experimental and revised the manuscript. All authors agreed to the final version of this manuscript.

■ REFERENCES

- [1] Awortwe, C., Makiwane, M., Reuter, H., Muller, C., Louw, J., and Rosenkranz, B., 2018, Critical evaluation of causality assessment of herb-drug interactions in patients, *Br. J. Clin. Pharmacol.*, 84 (4), 679–693.
- [2] Fasinu, P.S., Bouic, P.J., and Rosenkranz, B., 2012, An overview of the evidence and mechanisms of herb-drug interactions, *Front. Pharmacol.*, 3, 69.
- [3] Showande, S.J., Fayeke, T.O., Kajula, M., Hokkanen, J., and Tolonen, A., 2018, Potential inhibition of major human cytochrome P450 isoenzymes by selected tropical medicinal herbs-Implication for herb-drug interactions, *Food Sci. Nutr.*, 7 (1), 44–55.
- [4] Bo, L., Baosheng, Z., Yang, L., Mingmin, T., Beiran, L., Zhiqiang, L., and Huaqiang, Z., 2016, Herb-drug enzyme-mediated interactions, and the associated experimental methods: A review, *J. Tradit. Chin. Med.*, 36 (3), 392–408.
- [5] Buchman, C.D., Chai, S.C., and Chen, T., 2018, A current structural perspective on PXR and CAR in drug metabolism, *Expert Opin. Drug Metab. Toxicol.*, 14 (6), 635–647.
- [6] Daujat-Chavanieu, M., and Gerbal-Chaloin, S., 2020, Regulation of CAR and PXR expression in health and disease, *Cells*, 9 (11), 2395.
- [7] Wang, Y.M., Ong, S.S., Chai, S.C., and Chen, T., 2012, Role of CAR and PXR in xenobiotic sensing and metabolism, *Expert Opin. Drug Metab. Toxicol.*, 8 (7), 803–817.
- [8] Lynch, C., Mackowiak, B., Huang, R., Li, L., Heyward, S., Sakamuru, S., Wang, H., and Xia, M., 2018, Identification of modulators that activate the constitutive androstane receptor from the Tox21 10K compound library, *Toxicol. Sci.*, 167 (1), 282–292.
- [9] Hossain, M.S., Urbi, Z., Sule, A., and Rahman, K.M.H., 2014, *Andrographis paniculata* (Burm. f.) Wall. ex Nees: A Review of ethnobotany, phytochemistry, and pharmacology, *Sci. World J.*, 2014, 274905.
- [10] Kumar, S., Singh, B., and Bajpai, V., 2021, *Andrographis paniculata* (Burm.f.) Nees: Traditional uses, phytochemistry, pharmacological properties and quality control/quality assurance, *J. Ethnopharmacol.*, 275, 114054.
- [11] Dai, Y., Chen, S.R., Chai, L., Zhao, J., Wang, Y., and Wang, Y., 2019, Overview of pharmacological activities of *Andrographis paniculata* and its major compound andrographolide, *Crit. Rev. Food Sci. Nutr.*, 59 (Suppl. 1), S17–S29.
- [12] Kandanur, S.G.S., Tamang, N., Golakoti, N.R., and Nanduri, S., 2019, Andrographolide: A natural product template for the generation of structurally and biologically diverse diterpenes, *Eur. J. Med. Chem.*, 176, 513–533.
- [13] Balap, A., Lohidasan, S., Sinnathambi, A., and Mahadik, K., 2017, Herb-drug interaction of *Andrographis paniculata* (Nees) extract and andrographolide on pharmacokinetic and pharmacodynamic of naproxen in rats, *J. Ethnopharmacol.*, 195, 214–221.
- [14] Balap, A., Atre, B., Lohidasan, S., Sinnathambi, A., and Mahadik, K., 2016, Pharmacokinetic and

- pharmacodynamic herb-drug interaction of *Andrographis paniculata* (Nees) extract and andrographolide with etoricoxib after oral administration in rats, *J. Ethnopharmacol.*, 183, 9–17.
- [15] Chien, C.F., Wu, Y.T., Lee, W.C., Lin, L.C., and Tsai, T.H., 2010, Herb–drug interaction of *Andrographis paniculata* extract and andrographolide on the pharmacokinetics of theophylline in rats, *Chem. Biol. Interact.*, 184 (3), 458–465.
- [16] Pan, Y., Abd-Rashid, B.A., Ismail, Z., Ismail, R., Mak, J.W., Pook, P.C.K., Er, H.M., and Ong, C.E., 2011, In vitro determination of the effect of *Andrographis paniculata* extracts and andrographolide on human hepatic cytochrome P450 activities, *J. Nat. Med.*, 65 (3-4), 440–447.
- [17] Pekthong, D., Blanchard, N., Abadie, C., Bonet, A., Heyd, B., Manton, G., Berthelot, A., Richert, L., and Martin, H., 2009, Effects of *Andrographis paniculata* extract and andrographolide on hepatic cytochrome P450 mRNA expression and monooxygenase activities after *in vivo* administration to rats and *in vitro* in rat and human hepatocyte cultures, *Chem. Biol. Interact.*, 179 (2-3), 247–255.
- [18] Pekthong, D., Martin, H., Abadie, C., Bonet, A., Heyd, B., Manton, G., and Richert, L., 2008, Differential inhibition of rat and human hepatic cytochrome P450 by *Andrographis paniculata* extract and andrographolide, *J. Ethnopharmacol.*, 115 (3), 432–440.
- [19] Qiu, F., Hou, X.L., Takahashi, K., Chen, L.X., Azuma, J., and Kang, N., 2012, Andrographolide inhibits the expression and metabolic activity of cytochrome P450 3A4 in the modified Caco-2 cells, *J. Ethnopharmacol.*, 141 (2), 709–713.
- [20] Ooi, J.P., Kuroyanagi, M., Sulaiman, S.F., Tengku Muhammad, T.S., and Tan, M.L., 2011, Andrographolide and 14-Deoxy-11,12-didehydroandrographolide inhibit cytochrome P450s in HepG2 hepatoma cells, *Life Sci.*, 88 (9-10), 447–454.
- [21] Hafid, A.F., Rifai, B., Tumewu, L., Widiastuti, E., Dachliyati, L., Primaharinastiti, R., and Widyawaruyanti, A., 2015, Andrographolide determination of *Andrographis paniculata* extracts, ethyl acetate fractions and tablets by thin-layer chromatography, *J. Chem. Pharm. Res.*, 7 (12), 557–561.
- [22] Wang, J., Yang, W., Wang, G., Tang, P., and Sai, Y., 2014, Determination of six components of *Andrographis paniculata* extract and one major metabolite of andrographolide in rat plasma by liquid chromatography-tandem mass spectrometry, *J. Chromatogr. B*, 951-952, 78–88.
- [23] Liu, Y.H., Mo, S.L., Bi, H.C., Hu, B.F., Li, C.G., Wang, Y.T., Huang, L., Huang, M., Duan, W., Liu, J.P., Wei, M.Q., and Zhou, S.F., 2011, Regulation of human pregnane X receptor and its target gene cytochrome P450 3A4 by Chinese herbal compounds and a molecular docking study, *Xenobiotica*, 41 (4), 259–280.
- [24] Küblbeck, J., Niskanen, J., and Honkakoski, P., 2020, Metabolism-disrupting chemicals and the constitutive androstane receptor CAR, *Cells*, 9 (10), 2306.
- [25] Borse, S.P., Singh, D.P., and Nivsarkar, M., 2019, Understanding the relevance of herb-drug interaction studies with special focus on interplays: A prerequisite for integrative medicine, *Porto Biomed. J.*, 4 (2), e15.
- [26] Pitaloka, D.A.E., Ramadhan, D.S.F., Arfan, A., Chaidir, L., and Fakhri, T.M., 2021, Docking-based virtual screening and molecular dynamics simulations of quercetin analogs as enoyl-acyl carrier protein reductase (InhA) inhibitors of *Mycobacterium tuberculosis*, *Sci. Pharm.*, 89 (2), 20.
- [27] Pitaloka, D.A.E., Damayanti, S., Artarini, A.A., and Sukandar, E.Y., 2019, Molecular docking, dynamics simulation, and scanning electron microscopy (SEM) examination of clinically isolated *Mycobacterium tuberculosis* by ursolic acid: A pentacyclic triterpenes, *Indones. J. Chem.*, 19, (2), 328–336.
- [28] Shivanika, C., Deepak Kumar, S., Ragunathan, V., Tiwari, P., Sumitha, A., and Devi, P.B., 2020, Molecular docking, validation, dynamics simulations, and pharmacokinetic prediction of natural compounds against the SARS-CoV-2 main-protease, *J. Biomol. Struct. Dyn.*, 0 (0), 1–27.

- [29] Lee, H.S., Jo, S., Lim, H.S., and Im, W., 2012, Application of binding free energy calculations to prediction of binding modes and affinities of MDM2 and MDMX inhibitors, *J. Chem. Inf. Model.*, 52 (7), 1821–1832.
- [30] Maglich, J.M., Parks, D.J., Moore, L.B., Collins, J.L., Goodwin, B., Billin, A.N., Stoltz, C.A., Kliewer, S.A., Lambert, M.H., Willson, T.M., and Moore, J.T., 2003, Identification of a novel human constitutive androstane receptor (CAR) agonist and its use in the identification of CAR target genes, *J. Biol. Chem.*, 278 (19), 17277–17283.
- [31] Chen, J., and Raymond, K., 2006, Roles of Rifampicin in drug-drug interactions: underlying molecular mechanisms involving the nuclear pregnane X receptor, *Ann. Clin. Microbiol. Antimicrob.*, 5 (1), 3.
- [32] Chrencik, J.E., Orans, J., Moore, L.B., Xue, Y., Peng, L., Collins, J.L., Wisely, G.B., Lambert, M.H., Kliewer, S.A., and Redinbo, M.R., 2005, Structural disorder in the complex of human pregnane X receptor and the macrolide antibiotic Rifampicin, *Mol. Endocrinol.*, 19 (5), 1125–1134.
- [33] Damayanti, S., Martak, N.A.S., Permana, B., Suwandi, A., Hartati, R., and Wibowo, I., 2020, *In silico* study on interaction and preliminary toxicity prediction of *Eleutherine Americana* components as an antifungal and antitoxoplasmosis candidate, *Indones. J. Chem.*, 20 (4), 899–910.
- [34] Hollingsworth, S.A., and Dror, R.O., 2018, Molecular dynamics simulation for all, *Neuron*, 99 (6), 1129–1143.
- [35] Bao, L., Wang, J., and Xiao, Y., 2019, Molecular dynamics simulation of the binding process of ligands to the add adenine riboswitch aptamer, *Phys. Rev. E*, 100 (2), 022412.
- [36] Ravi, S., Priya, B., Dubey, P., Thiruvengatam, V., and Kirubakaran, S., 2021, Molecular docking and molecular dynamics simulation studies of quinoline-3-carboxamide derivatives with DDR kinases—selectivity studies towards ATM kinase, *Chemistry*, 3 (2), 511–524.
- [37] Bai, B., Zou, R., Chan, H.C.S., Li, H., and Yuan, S., 2021, MolADI: A web server for automatic analysis of protein-small molecule dynamic interactions, *Molecules*, 26 (15), 4625.
- [38] Dash, R., Ali, M.C., Dash, N., Azad, M.A.K., Hosen, S.M.Z., Hannan, M.A., and Moon, I.S., 2019, Structural and dynamic characterizations highlight the deleterious role of SULT1A1 R213H polymorphism in substrate binding, *Int. J. Mol. Sci.*, 20 (24), 6256.
- [39] Dewi, M.L., Fakhri, T.M., and Sofyan, R.I., 2021, The discovery of tyrosinase enzyme inhibitors activity from polyphenolic compounds in red grape seeds through in silico study, *J. Pure Appl. Chem. Res.*, 10 (2), 104–112.
- [40] Khanal, S.P., Koirala, R.P., Mishra, E., and Adhikari, N.P., 2021, Molecular dynamics study of structural properties of γ -aminobutyric acid (GABA), *BIBECHANA*, 18 (1), 67–74.
- [41] Zhang, X., Liu, X., He, M., Zhang, Y., Sun, Y and Lu, X, 2020, A molecular dynamics simulation study of KF and NaF ion pairs in hydrothermal fluIDs, *Fluid Phase Equilib.*, 518, 112625.
- [42] Levine, B.G., Stone, J.E., and Kohlmeyer, A., 2011, Fast analysis of molecular dynamics trajectories with graphics processing units—Radial distribution function histogramming, *J. Comput. Phys.*, 230 (9), 3556–3569.
- [43] Zikri, A.T., Pranowo, H.D., and Haryadi, W., 2020, Stability, hydrogen bond occupancy analysis and binding free energy calculation from flavonol docked in DAPK1 active site using molecular dynamics simulation approaches, *Indones. J. Chem.*, 21 (2), 383–390.
- [44] Subash, K.R., 2020, *In silico* pharmacokinetic and toxicological properties prediction of bioactive compounds from *Andrographis paniculata*, *Natl. J. Physiol., Pharm. Pharmacol.*, 10 (7), 537–542.
- [45] Julaiha, J., Widodo, G.P., and Herowati, R., 2019, Predicting ADME and molecular docking analysis of *Andrographis paniculata* and *Strobilanthes crispus* chemical constituents against antidiabetic molecular targets, *J. Idn. Chem. Soc.*, 2 (2), 66–125.
- [46] Lindawati, N.Y., Nugroho, A.E., and Pramono, S., 2015, Pengaruh kombinasi ekstrak terpurifikasi

- herba sambiloto (*Andrographis paniculata* (Burm. f.) Nees) dan herba pegagan (*Centella asiatica* (L.) Urban) terhadap translokasi protein GLUT-4 pada tikus diabetes mellitus tipe 2 resisten insulin, *Trad. Med. J.*, 19 (2), 62–69.
- [47] Nugroho, A.E., Rais, I.R., Setiawan, I., Pratiwi, P.Y., Hadibarata, T., Maulana, T., and Pramono, S., 2014, Pancreatic effect of andrographolide isolated from *Andrographis paniculata* (Burm. f.) Nees, *Pak. J. Biol. Sci.*, 17 (1), 22–31.
- [48] Samala, S. and Veeresham, C., 2015, Andrographolide pretreatment enhances the bioavailability and hypoglycemic action of glimepiride and metformin, *Int. J. Phytomed.*, 7 (3), 254–264.
- [49] Zhang, X., Zhang, X., Wang, X., and Zhao, M., 2018, Influence of andrographolide on the pharmacokinetics of warfarin in rats, *Pharm. Biol.*, 56 (1), 351–356.